

# Pretherapeutic functional neuroimaging predicts tremor arrest after thalamotomy

C. Tuleasca<sup>1,2,3,4</sup>  | E. Najdenovska<sup>2</sup> | J. Régis<sup>5</sup> | T. Witjas<sup>6</sup> | N. Girard<sup>7</sup> |  
J. Champoudry<sup>5</sup> | M. Faouzi<sup>8</sup> | J.-P. Thiran<sup>3,4,9</sup> | M. Bach Cuadra<sup>2,3</sup> | M. Levivier<sup>1,4</sup> |  
D. Van De Ville<sup>10,11</sup>

<sup>1</sup>Neurosurgery Service and Gamma Knife Center, Centre Hospitalier Universitaire Vaudois (CHUV), Lausanne, Switzerland

<sup>2</sup>Medical Image Analysis Laboratory (MIAL) and Department of Radiology-Center of Biomedical Imaging (CIBM), Centre Hospitalier Universitaire Vaudois, Lausanne, Switzerland

<sup>3</sup>Signal Processing Laboratory (LTS 5), Ecole Polytechnique Fédérale de Lausanne (EPFL), Lausanne, Switzerland

<sup>4</sup>Faculty of Biology and Medicine, University of Lausanne, Lausanne, Switzerland

<sup>5</sup>Stereotactic and Functional Neurosurgery Service and Gamma Knife Unit, CHU Timone, Marseille, France

<sup>6</sup>Neurology Department, CHU Timone, Marseille, France

<sup>7</sup>AMU, CRMBM UMR CNRS 7339, Faculté de Médecine et APHM, Department of Diagnostic and Interventional Neuroradiology, Hôpital Timone, Marseille, France

<sup>8</sup>Center for Clinical Epidemiology, Institute of Social and Preventive Medicine, Lausanne, Switzerland

<sup>9</sup>Department of Radiology, Centre Hospitalier Universitaire Vaudois, Lausanne, Switzerland

<sup>10</sup>Faculty of Medicine, University of Geneva, Geneva, Switzerland

<sup>11</sup>Medical Image Processing Laboratory, Ecole Polytechnique Fédérale de Lausanne (EPFL), Lausanne, Switzerland

## Correspondence

C. Tuleasca, Neurosurgery Service and Gamma Knife Center, Centre Hospitalier Universitaire Vaudois, Lausanne, Switzerland.

Email: constantin.tuleasca@gmail.com  
and

D. Van De Ville, Faculty of Medicine, University of Geneva, Geneva, Switzerland.  
Email: dimitri.vandeville@epfl.ch

## Funding information

This work has been supported by the Timone University Hospital, the Swiss National Science Foundation SNSF-205321-157040, the Centre d'Imagerie BioMédicale (CIBM) of the University of Lausanne (UNIL), the University of Geneva (UniGe), the Centre Hospitalier Universitaire Vaudois (CHUV), and the Leenaards and Jeantet Foundations.

**Objective:** Essential tremor (ET) represents the most common movement disorder. Drug-resistant ET can benefit from standard stereotactic procedures (deep brain stimulation or radiofrequency thalamotomy) or alternatively minimally invasive high-focused ultrasound or radiosurgery. All aim at same target, thalamic ventro-intermediate nucleus (Vim).

**Methods:** The study included a cohort of 17 consecutive patients, with ET, treated only with left unilateral stereotactic radiosurgical thalamotomy (SRS-T) between September 2014 and August 2015. The mean time to tremor improvement was 3.32 months (SD 2.7, 0.5-10). Neuroimaging data were collected at baseline (n = 17). Standard tremor scores, including activities of daily living (ADL) and tremor score on treated hand (TSTH), were completed pretherapeutically and 1 year later. We further correlate these scores with baseline inter-connectivity in twenty major large-scale brain networks.

**Results:** We report as predictive three networks, with the interconnected statistically significant clusters: primary motor cortex interconnected with inferior olivary nucleus<sup>1</sup>, bilateral thalamus interconnected with motor cerebellum lobule V<sup>2</sup> (ADL), and anterior default-mode network interconnected with Brodmann area 10<sup>3</sup> (TSTH). For all, more positive pretherapeutic interconnectivity correlated with higher drop in points on the respective scores. Age, disease duration, or time-to-response after

Najdenovska and Régis are equally contributors as second author.

Levivier and Van De Ville are equally contributors as last author.

SRS-T were not statistically correlated with pretherapeutic brain connectivity measures ( $P > .05$ ). The same applied to pretherapeutic tremor scores, after using the same methodology described above.

**Conclusions:** Our findings have clinical implications for predicting clinical response after SRS-T. Here, using pretherapeutic magnetic resonance imaging and data processing without prior hypothesis, we show that pretherapeutic network(s) interconnectivity strength predicts tremor arrest in drug-naïve ET, following stereotactic radiosurgical thalamotomy.

#### KEYWORDS

essential tremor, fMRI, resting state, stereotactic radiosurgery, thalamotomy

## 1 | INTRODUCTION

Essential tremor (ET) is the most common movement disorder.<sup>1</sup> Considered initially a mono-symptomatic disease of postural or action tremor, recent clinical, neuroimaging, and morphopathological studies<sup>2,3</sup> rather see ET as a multi-phenotype entity, with both motor and non-motor symptoms. Its main feature, tremor, is usually bilateral, predominant on upper extremities, with a frequency between 4 and 12 Hz.<sup>1</sup> An open question remains whether ET is of central or peripheral origin, and consequently the core role of the cerebellum versus the olivary complex has received great interest from the neuroscience community.<sup>4</sup> Additional use of non-invasive neuroimaging techniques<sup>5</sup> or findings from deep brain stimulation (DBS)<sup>6</sup> has pointed out toward an involvement of the so-called tremor network (contralateral cerebellum; ipsilateral motor thalamus; and primary motor cortex).

Currently, three different views on ET are under debate: abnormal oscillations within the tremor network, progressive cell loss in the frame of a neurodegenerative disorder, or a localized GABAergic dysfunction.<sup>5</sup>

Primary treatment is pharmacological.<sup>7</sup> Drug-resistant ET can benefit from standard functional neurosurgery procedures (DBS or radiofrequency thalamotomy)<sup>8</sup> or alternatively minimally invasive procedures, including radiosurgery (RS)<sup>9</sup> or high-focused ultrasound (HIFU).<sup>10</sup> All aim at the same target, the motor thalamus part called ventro-intermediate nucleus (Vim).

It is now well established that many diseases (including movement disorders) can be characterized by alterations in functional networks, which are spatially distant brain regions that interact to support brain function.<sup>2,11</sup> Seminal work of Biswal et al<sup>12</sup> demonstrated that during rest, blood-oxygen-level-dependent (BOLD) time-series, both primary motor areas exhibit a high correlation. Since then, several methodologies to extract functional connectivity or interconnectivity—if within a functional network—have been proposed to measure temporal dependencies of neuronal activation between anatomically separated brain regions.

Here, we performed pretherapeutic resting-state fMRI in 17 patients, to clarify which networks and the statistically significant intercorrelated anatomical clusters would best correlate with clinical

improvement, 1 year after stereotactic radiosurgical thalamotomy (SRS-T, having delayed clinical effect [mean 4 months, going up to 1 year]).<sup>9,13</sup>

## 2 | MATERIALS AND METHODS

### 2.1 | Study design

Participants were part of the ongoing, prospective, longitudinal neuroimaging trial of SRS-T for tremor, in CHU Timone, Marseille, France. Our data with regard to safety and efficacy of SRS-T have already been published (see Witjas et al<sup>9</sup>). Ethical Committee of the Timone University Hospital (CPPRB 1) gave formal approval. Written informed consent was obtained from all patients.

A cohort of included 17 consecutive patients (only right-sided, drug-resistant) treated only with left unilateral SRS-T between September 2014 and August 2015. All were referred by neurologist specialized in movement disorders (TW). Clinical diagnosis was ET in all cases. Patients were excluded if previous contralateral thalamotomy, epilepsy, vascular ischemic events, organic lesions, etc., which might have affected resting-state fMRI networks.

No patient was under tremor medication during the functional neuroimaging study protocol.

Patients meeting inclusion criteria undertook screening visit, including baseline tremor assessment (by TW) and neuroimaging, with structural MRI and resting-state fMRI (Siemens Skyra, 3 Tesla, Munich, Germany; see below). An identical clinical protocol for tremor evaluation had been used 1 year after SRS-T. Basic demographic data can be found in Table 1.

The mean age was 70.1 years (range 49–82). Upper age limit for inclusion in the protocol is 80 years old. One exception was made since 2014 (beginning of the trial), for a 82-years-old patient, with good quality of life (except the tremor aspect).

### 2.2 | Tremor assessment

Tremor severity was assessed using questionnaire designed by Bain et al<sup>14</sup> (eg, activities of daily living [ADL])<sup>14</sup> and tremor score on the

**TABLE 1** Demographic data

Variable	Mean	SD	Minimum	Maximum
Duration of symptoms (y)	38	19.5	6	70
Age (y)	70.1	9.8	49	82
ADL baseline (points)	29.1	12	13	49
ADL (drop in points, 1 y minus baseline)	-23.06	11.9	2	-45
Tremor score on the treated hand (TSTH) baseline	18.6	5.5	8	30
(TSTH) (drop in points, 1 y minus baseline)	-11.4	4.1	-4	-19
Time to improvement after Vim RS (mo)	3.3	2.7	0.5	10

right treated hand, from "Fahn-Tolosa-Marin tremor rating scale"<sup>15</sup> (Table 2).

### 2.3 | Stereotactic radiosurgical thalamotomy procedure

Stereotactic radiosurgical thalamotomies were performed by same neurosurgeon (JR). After application of Leksell<sup>®</sup> coordinate G Frame (Elekta AB, Stockholm, Sweden), under local anesthesia,<sup>16</sup> all patients underwent both stereotactic CT and MRI. Indirect targeting was performed in all cases using identical methodology by Guiot's diagram,<sup>17</sup> single 4-mm isocenter and maximal prescription dose of 130 Gy.

### 2.4 | fMRI data acquisition and preprocessing

Imaging was performed on a head-only 3T magnetic resonance imaging (MRI) scanner, SIEMENS SKYRA (Siemens Medical Solutions). For T2\*-weighted fast echo planar imaging (BOLD contrast) were used TR/TE = 3.3 s/30 ms/90°, voxel size 4 × 4 × 4 mm,<sup>3</sup> 300 volumes acquired per subject, 46 interleaved axial slices. The rs-fMRI experiments, acquired with no explicit task, consisted of a 10-minutes run, in which participant was asked to relax with their eyes closed, without falling asleep or engaging in cognitive or motor tasks. In

addition, a field map was acquired to correct for the effect of field inhomogeneity.

Imaging data were analyzed in Lausanne (Switzerland), by two persons not involved in patient selection, treatment, or post-therapeutic evaluation (CT, DVDV). Processing of fMRI data was performed using standard software suites, SPM12 (<http://www.fil.ion.ucl.ac.uk/spm/>). Functional scans were realigned to the first scan of the series. After frame censoring in relation to motion (see below, frame censoring), the remaining time-points were spatially normalized into the standard anatomical space as defined by the Montreal Neurological Institute (SPM-MNI) and spatially smoothed using a Gaussian filter with a full width at high maximum (FWHM) of 6 mm. The voxel size generated from the above acquisition parameters was oversampled to 2 × 2 × 2 mm<sup>3</sup>.

### 2.5 | Frame censoring

Head motion during the MRI acquisitions, even if of submillimetric amplitude, has been already demonstrated as non-physiological source of spurious brain connectivity in resting-state fMRI data.<sup>18,19</sup> We computed Power's framewise displacement index for each time point.<sup>18</sup> When it exceeded 0.5 mm, the corresponding frame was "scrubbed" along with one preceding and two following ones (for a total of 5 for one time-point exceeding the upper limit allowed). Only the remaining frames were further considered for analysis. In the present cohort, the mean number of frames taken out was 35 (median 15, range 0-135).

### 2.6 | Resting-state networks extraction

Group-level independent component analysis (ICA) was applied to decompose the fMRI data into networks of temporally coherent spontaneous activity using the GIFT Toolbox (<http://icatb.sourceforge.net>).<sup>20</sup> The concat-ICA approach is data-driven and considers the concatenated data of 17 scans.<sup>21</sup> The total number of independent components (ICs) was set to 20, which is common setting in literature to identify large-scale distributed networks (Figures 1 and 2). Visual inspection of IC maps revealed neurological meaningful patterns; no components were excluded for further analysis.

**TABLE 2** The pertinent network with the corresponding interconnected relevant anatomical cluster, as well as the Montreal Neurological Institute (MNI) coordinates, the corresponding corrected p value after family-wise error (FWE) correction, the size of the cluster (Kc), and the peak level of the former

Network	Interconnectivity between the network and the relevant anatomical cluster	MNI	p FWE corrected	Kc	Peak level
Network 12	Inferior olivary nucleus (correlates with ADL improvement)	0, -26, -42 -6, -34, -40	0.015	62	35.30 27.54
Network 13	Right and left motor cerebellum lobule V (correlates with ADL improvement)	6, -58, -10 -4, -62, -16	0.000	135	51.82 45.09
Network 14	Right rostral prefrontal cortex (BA 10) (correlates with TSTH improvement)	22, 58, 18	0.005	79	41.59



### Large-scale distributed networks (n1-n10) as extracted from baseline resting-state fMRI

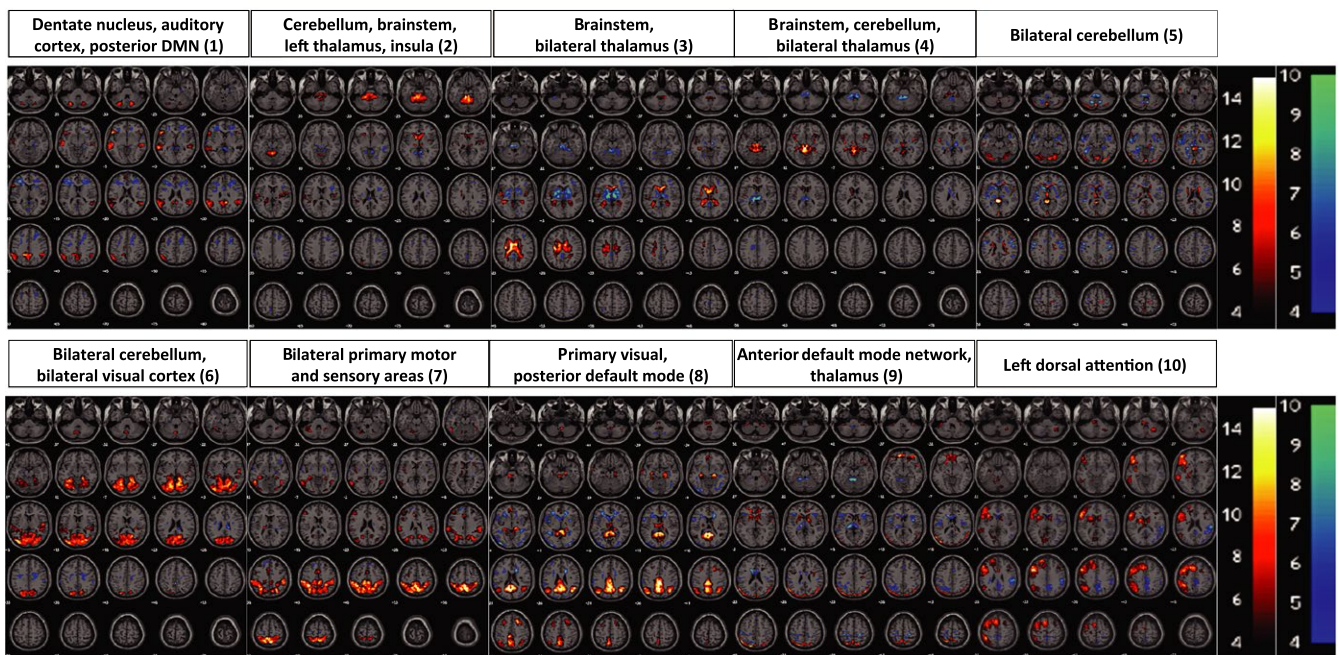


**FIGURE 1** Set of large-scale brain networks obtained from pretherapeutic resting-state fMRI (networks 1-10)

### Large-scale distributed networks (n11-n20) as extracted from baseline resting-state fMRI

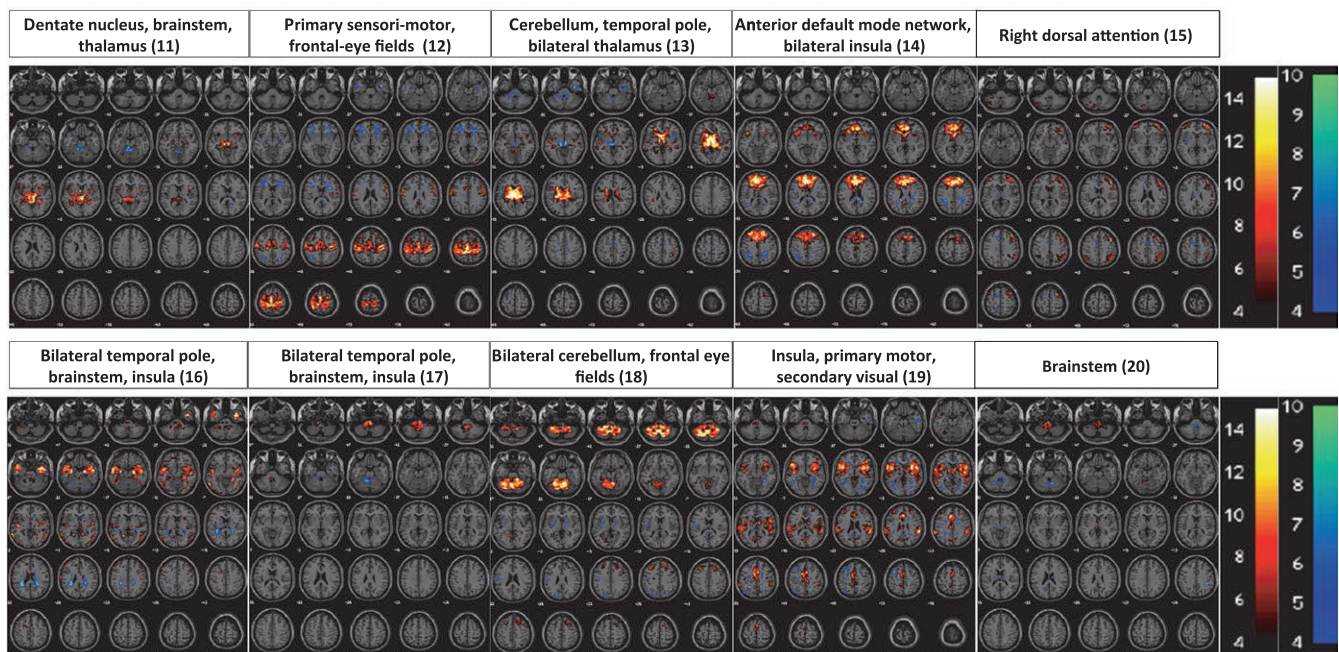


**FIGURE 2** Set of large-scale brain networks obtained from pretherapeutic resting-state fMRI (networks 11-20)

## 2.7 | Statistical analysis

For rs-fMRI data, analysis of variance (ANOVA) was implemented in SPM12 as a *flexible factorial model*. This analysis was made on each component,

using the individual subject-level maps. As we wanted to apply the model to each component, we used a Bonferroni correction to deal with number of models (20). Within each model, we then report corrected *P*-values using conventional cluster-level family-wise error (FWE) correction (Table 2).

### 3 | RESULTS

#### 3.1 | Large-scale functional networks during resting state

A set of 20 networks spanning the whole brain (see Materials and Methods) was identified. Independent components (networks) were defined using the baseline scans of all subjects, and subject-dependent maps were retrieved using conventional regression. After visual inspection of the maps at the group level, all components showed neurologically relevant spatial patterns and were kept for subsequent analysis (Figures 1 and 2).

#### 3.2 | Linking functional networks at baseline to changes in standard clinical scores

For each component, subject-level spatial maps that represent strength of interconnectivity in a large-scale network at baseline were fed into general linear model that included the difference in points for ADL and TSTH between 1 year after SRS-T and baseline pretherapeutic values. This allowed assessing whether voxels correlated significantly with tremor improvement. Within each linear model, we use cluster-level Gaussian random field theory to correct for testing whole-brain voxels, but, as the linear model is applied to each component separately, we also additionally applied Bonferroni correction to deal with multiple comparisons (20) and report corrected *P*-values.

We report three networks, which revealed statistical significant clusters. For ADL improvement, we found network 12 (bilateral motor network, frontal eye-fields) and network 13 (bilateral thalamus, cerebellum); for TSTH improvement, network 14 (bilateral insula, mesial prefrontal cortex).

For network 12, we found a significant cluster within and adjacent to inferior olivary nucleus (ION, Figures 3 and 5, Table 2). The more positive interconnectivity at baseline, the higher the drop in points on the ADL score. This result thus represents connectivity between bilateral motor cortex and frontal eye-fields and the ION.

For network 13, we found significant clusters within right (predominant) and left motor cerebellum lobule V (Figures 3 and 5, Table 2). The more positive interconnectivity at baseline, the higher drop in points on the ADL score. This result thus represents connectivity between the bilateral thalamus and right motor cerebellum lobule V.

For network 14, we found significant clusters within right medial rostral prefrontal cortex, known as right Brodmann area 10 (BA 10, Figures 4 and 5, Table 2). The more positive interconnectivity at baseline, the higher drop in points on TSTH score. This result thus represents connectivity between anterior default-mode network and bilateral insula with the right BA 10.

#### 3.3 | Assessment of possible confounds

To exclude possible confounders, using the same methodology, no statistically significant cluster was found while assessing correlations with the pretherapeutic tremor scores. This was of particular interest to exclude a relationship between baseline scores and their respective drop in points 1 year later, which could have been reflected in our results.

Furthermore, age, disease duration, or time-to-response after SRS-T were not statistically correlated with baseline brain interconnectivity measures (Spearman's rank correlation coefficient  $>0.05$ , using Stata version 11; Stata Corp LLC, College stations, TX, USA).

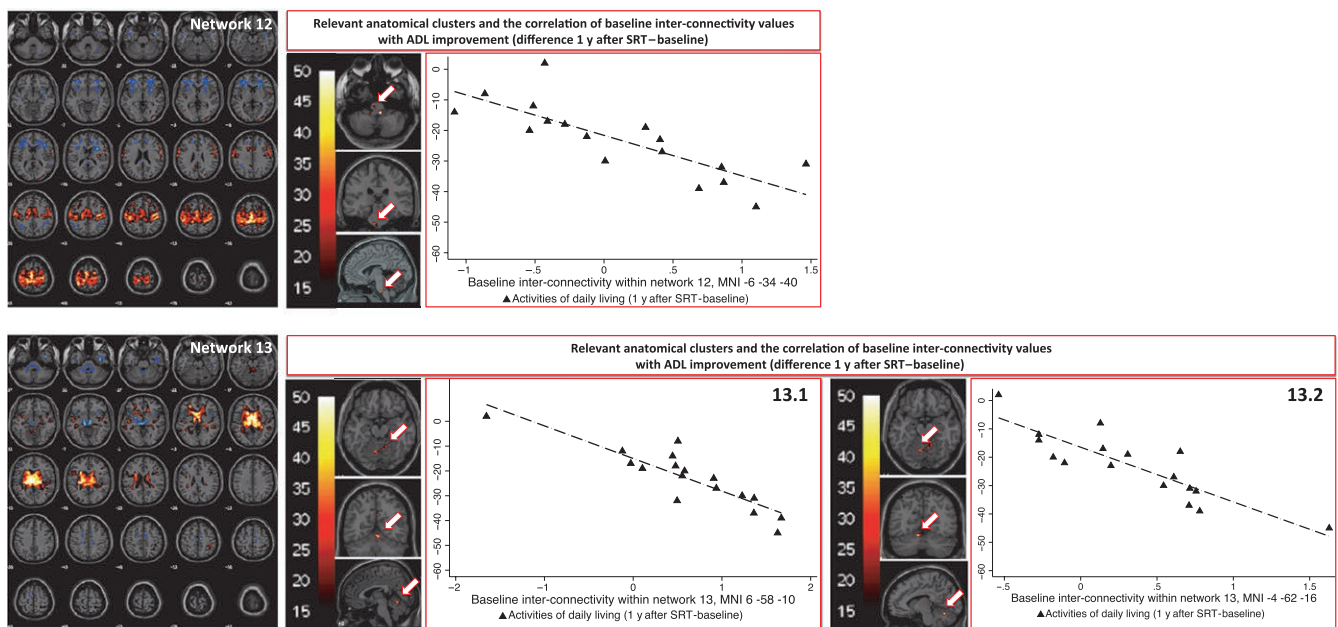


**FIGURE 3** Correlation between brain interconnectivity values and drop in ADL: interconnectivity between network 12 and inferior olivary nucleus and between network 13 and right (13.1) and left (13.2) cerebellum lobule V. SRT, stereotactic radiosurgical thalamotomy



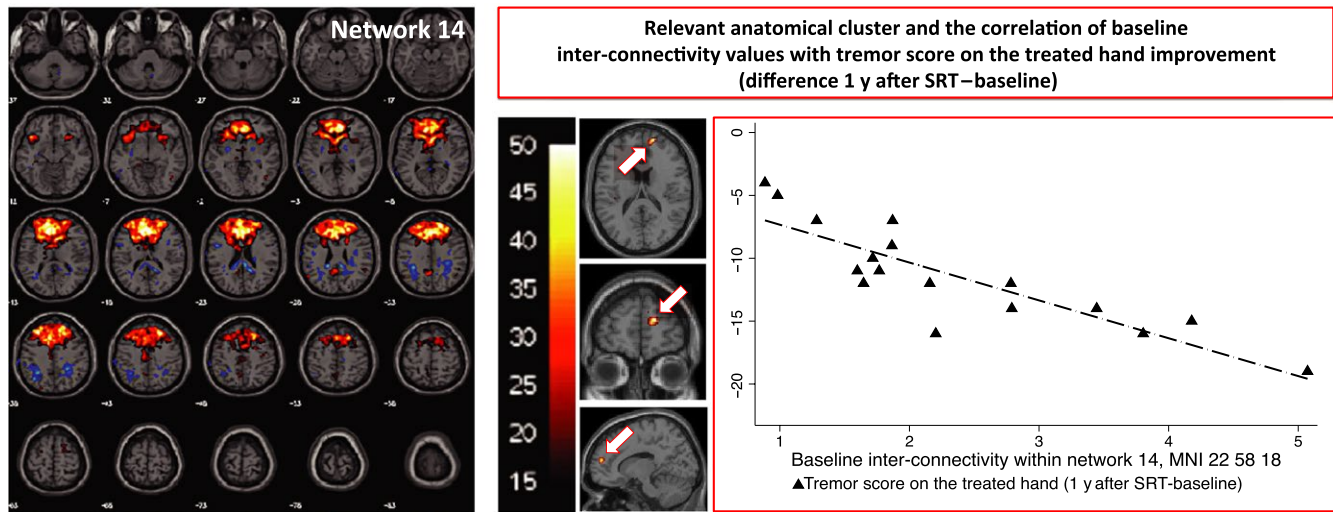


**FIGURE 4** Correlation between brain interconnectivity values and drop in TSTH: interconnectivity between network 14 and mesial aspect of Brodmann area 10. SRT, stereotactic radiosurgical thalamotomy

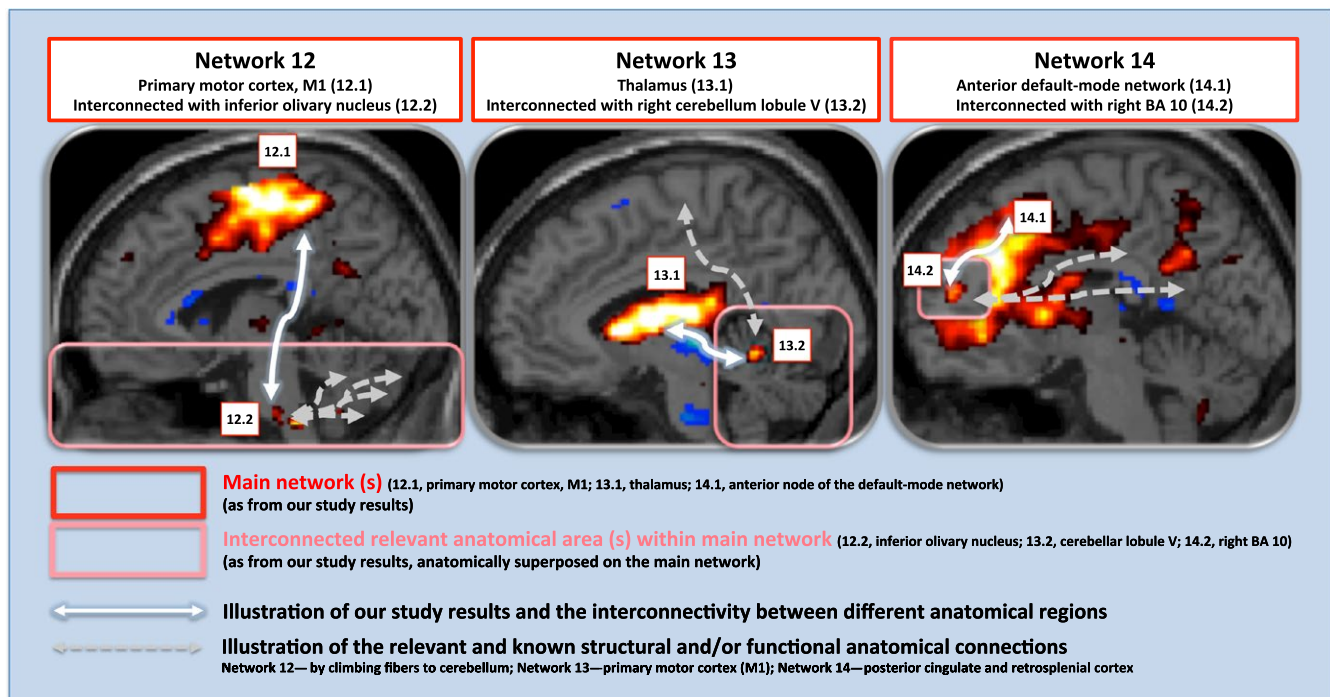


**FIGURE 5** Schematic illustration of the main findings in the present study. They are based upon real fMRI findings, superposed on a structural imaging, for an easier visualization

### 3.4 | Radiological answer: MR signature after thalamotomy (1 year after SRS-T)

Mean MR signature volume after SRS-T was 125 mm<sup>3</sup> (SD 162, 2-600 mm<sup>3</sup>). This was drawn individually on T1 Gadolinium-injected MR, 1 year after SRS-T, considered definitive radiological answer in our experience.<sup>9</sup> To ensure volume calculation accuracy, each patient MR (1 year after SRS-T) was imported in Leksell GammaPlan software (LGP; Elekta instruments, AB, Sweden). This was co-registered with therapeutic images. The 90 Gy isodose

line, which corresponds to final MR signature in our experience,<sup>9,22</sup> was projected to the 1-year result and matched perfectly the MR signature. Manually, using LGP segmentation tools, volume was individually drawn and further automatically calculated by the software.

There was no correlation between thalamotomy volume and ADL drop ( $P > .05$ ), but there was with TSTH drop ( $P = .01$ ).

None of the baseline IC values reported within the significant clusters showed statistically significant correlation with thalamotomy volume ( $P > .05$ ).

## 4 | DISCUSSION

Essential tremor is a disabling neurological disorder that has a major impact on quality of life and comes with a significant psychological burden for patients.<sup>1</sup> Despite numerous studies and advances in both neuroimaging and neuropathology, our insights in underlying mechanisms are still limited,<sup>1</sup> with an ongoing debate concerning the role of the ION versus the cerebellum in disease generation and progression. During the past two decades, new developments in neuroimaging techniques, including structural (diffusion tensor imaging<sup>23</sup>) and functional (resting-state fMRI, PET<sup>2,24</sup>) data, have become increasingly used to evaluate movements disorders pathophysiology, with minimal patients compliance, mainly in ET and Parkinson's disease. Electrophysiological studies have additionally shed new light, while exploring the electrical activity of key anatomical structures, such as the subthalamic nucleus, by microelectrode recording, together with electromyograms, as in the recent study of Li et al.<sup>25</sup>

Our findings reveal, for the first time, that functional network measures, extracted from pretherapeutic resting-state fMRI at baseline, relate to drop in standard tremor scores 1 year after SRS-T, for both ADL and TSTH. For ADL improvement, the inferior olivary nucleus showed higher interconnectivity with network including bilateral motor cortex and frontal eye-fields, as well as motor cerebellum lobule V with the network constituted by bilateral thalamus. For TSTH improvement, right mesial aspect of Brodmann area 10 showed higher interconnectivity with anterior default-mode network and bilateral insula. Of note, ADL is a global tremor score, involving many aspects, while TSTH is only related to a specific aspect (eg, the hand). In this sense, neuroimaging distinction of two different clinical evaluations is not necessarily astonishing.

We briefly prompt the pertinent roles of each involved functional networks. The first network (network 12 in our study) encompasses bilateral motor cortex and frontal eye-fields, interconnected with left inferior olivary nucleus. The involvement of so-called tremor network in tremor generation has been sustained by numerous neuroimaging studies.<sup>5</sup> The role of inferior olivary nucleus versus cerebellum has been debated for decades as being main actor in ET's pathogenesis. Louis et al<sup>26</sup> have performed a systematic post-mortem study of microscopic changes in inferior olivary nucleus and did not detect any structural differences between ET cases and healthy matched controls. The same applied for functional neuroimaging positron emission tomography studies, which failed to identify any metabolic activity at this level.<sup>27</sup> Both have pointed out toward the conclusion that if inferior olivary nucleus is involved in ET, there is no structural or metabolic modification.<sup>26</sup> Furthermore, Bucher et al<sup>28</sup> used fMRI to study possible cerebral activation patterns associated with unilateral postural tremor; the authors concluded that ET is mainly associated with an additional contralateral cerebellar pathway activation and overactivity in cerebellum, red nucleus, and globus pallidus, without significant intrinsic olivary activation. However, an isolated fMRI case-report, after opened surgical radiofrequency thalamotomy, revealed significant activation within inferior olivary nucleus after surgery.<sup>29</sup> It is worth noting that historically, based upon oscillatory-pacemaking

properties, inferior olivary nucleus has been proposed as primary driver of ET pathogenesis due to its implication in learning and timing of motor behavior,<sup>30</sup> meaning an involvement in control and coordination of movements, sensory processing, and cognitive tasks, probable by encrypting timing of sensory input independently of attention or awareness. Two types of input are particularly of interest: one allowing for movement learning (actions), and other for posture and balance maintaining (maintenance reflexes),<sup>31</sup> which could be relevant in the context of patients with ET. There are four major electrophysiological theories about the role of the inferior olivary nucleus: timing, learning, comparator, and "network oscillations." Timing theory (Welsh et al<sup>32</sup>) suggests the existence of an oscillatory clock, offering proper scheduling of command signals for appropriate motor domains; same was supported by Yarom and Cohen,<sup>33</sup> considering motor deficits or tremor appearance as a manifestation of a damaged timing mechanism. Consequently, ET would reflect maladjustment in timing of muscle activation. Learning theory states that climbing fibers to the inferior olive provide the cerebellar Purkinje cells with an error signal indicating an eventual scarce motor activity. Comparator theory postulates that climbing fibers of inferior olive provide cerebellar Purkinje cells with a signal error that indicates inadequate motor activity. "Network oscillations" theory, suggested by Yarom and Cohen,<sup>33</sup> states that each neuron by itself cannot exhibit oscillatory behavior, but only when a network of electronically coupled neurons is formed.

The second network (network 13) encompasses bilateral thalamus and tremor drop relates to higher interconnectivity with bilateral (right predominance) motor cerebellum lobule V. In humans, DBS<sup>8</sup> or radiofrequency thalamotomy<sup>34</sup> of the cerebellar thalamic nucleus (ie, Vim) induces tremor arrest.<sup>35</sup> Additional findings from resting-state fMRI studies suggest that the cerebellar thalamus and the cerebellum are involved in the mechanism of ET.<sup>36</sup> Data from electrophysiology (Hua et al<sup>37</sup>), after single neurons awake mapping of the ventral thalamus in patients with ET prior to open radiofrequency thalamotomy, suggested that during tremor, Vim had a significantly higher proportion of "tremor neurons" compared to other thalamic areas. These findings were considered inconsistent with the olivo-cerebellar model previously described, which supposes motor cortex been driven through thalamic connections (which would be a combination of networks 12 and 13 in the present study). Schnitzer et al<sup>38</sup> used magnetoencephalography and revealed a motor network involving the contralateral primary motor cortex, premotor cortex, thalamus, brainstem, and ipsilateral cerebellum. A meta-analysis of neuroimaging studies<sup>39</sup> revealed that sensorimotor tasks activated the anterior lobule V (and adjacent lobule VI), with additional foci in lobule VIII. Lobule V is mainly associated with motor control. Furthermore, motor and somatosensory representations show largely overlapping activation patterns, with major cluster focused in lobule V.<sup>39</sup> The motor and somatosensory coordinates were right lateralized, in patients with right-handed tasks (as in the present study, right-hand tremor and right lobule V activation), consistent with established ipsilateral cerebellar somatotopy and homunculi.<sup>39</sup>

The third network (network 14) includes anterior default-mode network and bilateral insula; interconnectivity of right mesial aspect

of Brodmann area 10 relates to drop in tremor score on the treated hand. This area is relevant for cognitive tasks and by extension non-motor features in ET. Brodmann area 10 is considered as the only prefrontal area that has predominant interconnections with the supramodal cortex in prefrontal cortex (corresponding to network 14), anterior temporal, or cingulate cortex. Functionally, Semendeferi et al<sup>40</sup> advocated for a specific increase in connectivity, especially with other high-order association areas, underlying the role in initiative taking and the planning of future actions, trademarks of human behavior. Ramnani et al<sup>41</sup> stated that due to its particular connectivity patterns, would additionally play a crucial role in highest level of integration of multiple sensory modalities, coming from auditory, visual, and somatic sensory systems, which would help to integrate outcomes from multiple cognitive operations. Gilbert et al<sup>42</sup> have designed a “conjunction-type” fMRI study using a series of tasks that measure the construct of interest. Brodmann area 10 was activated when people switched from either stimulus-oriented to stimulus-independent attending. The authors suggested that medial BA 10 (as in our findings) is involved in promoting attention toward the external environment, as, for example, in situations that require a particularly fast response to external stimuli. The former is in line with the “gateway attentional hypothesis,” according to which BA 10 as a whole plays a major role in situations that demand subjects to bias attention between current sensory input and internally generated thought processes.

Although we have taken many precautions, there are several limitations that will need to be addressed by further research. Our results are statistically strong despite the relatively small sample size, and the relatively strong correlation that is retrieved. Of course, further validation in a larger and independent sample remains to be carried out to potentially establish a new marker for individualized prognosis of tremor score change. In addition, the neurological evaluation was not blinded. Likewise, the same could be applied to a set of preoperative data before open surgical radiofrequency thalamotomy or HIFU, which would give additional insights into the pathophysiology of ET and tremor arrest. We have additionally assessed the role of potential confounders (see Results section).

The real central node of ET remains to be established, while two alternative theories could be supported by our results. A pacemaker theory, with three possible anatomical sites: the left inferior olivary nucleus, the right cerebellar lobule V or the BA 10, as well as the components with whom they share interconnectivity, including the motor network, the thalamus, or the anterior node of the default-mode network and insula. This does not answer the dilemma whether the cerebellum versus the inferior olivary would be the central core of the disease. A network theory would advocate for the presence of one versus multiple networks, of whom one coupling motor cortex with the ION, the second the thalamus with motor cerebellum, and a third between the anterior default-mode network and bilateral insula and the BA10. Whether the former act in synchrony or disassociated remains to establish.

In light of what has been described above, one could suppose that the eventual oscillatory regulator in ET should have a resetting

mechanism. It is most probably that by stimulation (such as DBS) or ablative (such as radiofrequency thalamotomy, SRS-T or HIFU) procedures, this regulator stops ticking at the appropriate time. Furthermore, it gives a new onset, occurrence, and terminations within the system's oscillations, under a new neuronal control.

Our results suggest that pretherapeutic resting-state fMRI is informative about tremor improvement or arrest after SRS-T. The clear implications of both inferior olivary nucleus and motor cerebellum in tremor arrest are suggested. Furthermore, non-motor, cognitive areas, such as BA 10, are found to play a role. Our method was not specifically designed to support existing physiopathological theories, and thus these findings shed new light on the implication of networks and their alterations on tremor generation.

## ACKNOWLEDGEMENTS

We would like to thank to all the patients, for their willingness to take part of the present study. To Axelle Cretol, for her continuous support and updating of the database on regular basis; to Jérôme Champoudry, for the easy access to all the encoded radiological files.

## CONFLICT OF INTEREST

No conflict of interest.

## ORCID

C. Tuleasca  <http://orcid.org/0000-0001-6776-1486>

## REFERENCES

- Louis ED. Essential tremor. *Lancet Neurol.* 2005;4:100-110.
- Benito-Leon J, Louis ED, Romero JP, et al. Altered functional connectivity in essential tremor: a resting-state fMRI study. *Medicine.* 2015;94:e1936.
- Louis ED, Honig LS, Vonsattel JP, Maraganore DM, Borden S, Moskowitz CB. Essential tremor associated with focal nonnigral Lewy bodies: a clinicopathologic study. *Arch Neurol.* 2005;62:1004-1007.
- Deuschl G, Elble R. Essential tremor—neurodegenerative or nondegenerative disease towards a working definition of ET. *Mov Disord.* 2009;24:2033-2041.
- Sharifi S, Nederveen AJ, Booij J, van Rootselaar AF. Neuroimaging essentials in essential tremor: a systematic review. *Neuroimage Clin.* 2014;5:217-231.
- Hubble JP, Busenbark KL, Wilkinson S, et al. Effects of thalamic deep brain stimulation based on tremor type and diagnosis. *Mov Disord.* 1997;12:337-341.
- Louis ED. Treatment of medically refractory essential tremor. *N Engl J Med.* 2016;375:792-793.
- Benabid AL, Pollak P, Gao D, et al. Chronic electrical stimulation of the ventralis intermedius nucleus of the thalamus as a treatment of movement disorders. *J Neurosurg.* 1996;84:203-214.
- Witjas T, Carron R, Azulay JP, Regis J. Gammaknife thalamotomy for intractable tremors: clinical outcome and correlations with neuroimaging features. Paper presented at: MDS 17th International Congress of Parkinson's Disease and Movement Disorders 2013.



10. Lipsman N, Schwartz ML, Huang Y, et al. MR-guided focused ultrasound thalamotomy for essential tremor: a proof-of-concept study. *Lancet Neurol.* 2013;12:462-468.
11. Horn A, Reich M, Vorwerk J, et al. Connectivity Predicts deep brain stimulation outcome in Parkinson disease. *Ann Neurol.* 2017;82:67-78.
12. Biswal B, Yetkin FZ, Haughton VM, Hyde JS. Functional connectivity in the motor cortex of resting human brain using echo-planar MRI. *Magn Reson Med.* 1995;34:537-541.
13. Kondziolka D, Ong JG, Lee JY, Moore RY, Flickinger JC, Lunsford LD. Gamma Knife thalamotomy for essential tremor. *J Neurosurg.* 2008;108:111-117.
14. Bain PG, Findley LJ, Atchison P, et al. Assessing tremor severity. *J Neurol Neurosurg Psychiatry.* 1993;56:868-873.
15. Fahn S, Tolosa E, Marin C. Clinical rating scale for tremor. *Parkinson's Dis Mov Disord.* 1988;000:225-234.
16. Witjas T, Carron R, Krack P, et al. A prospective single-blind study of Gamma Knife thalamotomy for tremor. *Neurology.* 2015;85:1562-1568.
17. Guiot G, Arfel G, Derome P, Kahn A. Neurophysiologic control procedures for stereotaxic thalamotomy. *Neurochirurgie.* 1968;14:553-566.
18. Power JD, Barnes KA, Snyder AZ, Schlaggar BL, Petersen SE. Spurious but systematic correlations in functional connectivity MRI networks arise from subject motion. *NeuroImage.* 2012;59:2142-2154.
19. Van Dijk KR, Sabuncu MR, Buckner RL. The influence of head motion on intrinsic functional connectivity MRI. *NeuroImage.* 2012;59:431-438.
20. Calhoun VD, Adali T, Pearlson GD, Pekar JJ. A method for making group inferences from functional MRI data using independent component analysis. *Hum Brain Mapp.* 2001;14:140-151.
21. Stone JV. Independent component analysis: an introduction. *Trends Cogn Sci.* 2002;6:59-64.
22. Régis J, Carron R, Park M. Is radiosurgery a neuromodulation therapy? A 2009 Fabrikant award lecture. *J Neurooncol.* 2010;98:155-162.
23. Lenfeldt N, Holmlund H, Larsson A, Birgander R, Forsgren L. Frontal white matter injuries predestine gait difficulties in Parkinson's disease. *Acta Neurol Scand.* 2016;134:210-218.
24. Buijink AW, van der Stouwe AM, Broersma M, et al. Motor network disruption in essential tremor: a functional and effective connectivity study. *Brain.* 2015;138:2934-2947.
25. Li X, Zhuang P, Hallett M, Zhang Y, Li J, Li Y. Subthalamic oscillatory activity in parkinsonian patients with off-period dystonia. *Acta Neurol Scand.* 2016;134:327-338.
26. Louis ED, Babij R, Cortes E, Vonsattel JP, Faust PL. The inferior olivary nucleus: a postmortem study of essential tremor cases versus controls. *Mov Disord.* 2013;28:779-786.
27. Wills AJ, Jenkins IH, Thompson PD, Findley LJ, Brooks DJ. Red nuclear and cerebellar but no olivary activation associated with essential tremor: a positron emission tomographic study. *Ann Neurol.* 1994;36:636-642.
28. Bucher SF, Seelos KC, Dodel RC, Reiser M, Oertel WH. Activation mapping in essential tremor with functional magnetic resonance imaging. *Ann Neurol.* 1997;41:32-40.
29. Hesselmann V, Maarouf M, Hunsche S, et al. Functional MRI for immediate monitoring stereotactic thalamotomy in a patient with essential tremor. *Eur Radiol.* 2006;16:2229-2233.
30. De Zeeuw CI, Simpson JI, Hoogenraad CC, Galjart N, Koekoek SK, Ruigrok TJ. Microcircuitry and function of the inferior olive. *Trends Neurosci.* 1998;21:391-400.
31. Marr D. A theory of cerebellar cortex. *J Physiol.* 1969;202:437-470.
32. Welsh JP, Lang EJ, Sugihara I, Llinas R. Dynamic organization of motor control within the olivocerebellar system. *Nature.* 1995;374:453-457.
33. Yarom Y, Cohen D. The olivocerebellar system as a generator of temporal patterns. *Ann N Y Acad Sci.* 2002;978:122-134.
34. Goldman MS, Ahlskog JE, Kelly PJ. The symptomatic and functional outcome of stereotactic thalamotomy for medically intractable essential tremor. *J Neurosurg.* 1992;76:924-928.
35. Campbell AM, Glover J, Chiang VL, Gerrard J, Yu JB. Gamma knife stereotactic radiosurgical thalamotomy for intractable tremor: a systematic review of the literature. *Radiother Oncol.* 2015;114:296-301.
36. Fang W, Chen H, Wang H, et al. Essential tremor is associated with disruption of functional connectivity in the ventral intermediate Nucleus-Motor Cortex-Cerebellum circuit. *Hum Brain Mapp.* 2016;37:165-178.
37. Hua SE, Lenz FA. Posture-related oscillations in human cerebellar thalamus in essential tremor are enabled by voluntary motor circuits. *J Neurophysiol.* 2005;93:117-127.
38. Schnitzler A, Munks C, Butz M, Timmermann L, Gross J. Synchronized brain network associated with essential tremor as revealed by magnetoencephalography. *Mov Disord.* 2009;24:1629-1635.
39. Stoodley CJ, Schmahmann JD. Functional topography in the human cerebellum: a meta-analysis of neuroimaging studies. *NeuroImage.* 2009;44:489-501.
40. Semendeferi K, Armstrong E, Schleicher A, Zilles K, Van Hoesen GW. Prefrontal cortex in humans and apes: a comparative study of area 10. *Am J Phys Anthropol.* Mar 2001;114:224-241.
41. Ramnani N, Owen AM. Anterior prefrontal cortex: insights into function from anatomy and neuroimaging. *Nat Rev Neurosci.* 2004;5:184-194.
42. Gilbert SJ, Frith CD, Burgess PW. Involvement of rostral prefrontal cortex in selection between stimulus-oriented and stimulus-independent thought. *Eur J Neurosci.* 2005;21:1423-1431.

**How to cite this article:** Tuleasca C, Najdenovska E, Régis J, et al. Pretherapeutic functional neuroimaging predicts tremor arrest after thalamotomy. *Acta Neurol Scand.* 2018;137:500–508. <https://doi.org/10.1111/ane.12891>